Third International Symposium on Marine Propulsors
smp'13, Launceston, Tasmania, Australia, May 2013

Numerical Analysis of Unsteady Open Water Characteristics of Surface Piercing Propeller

Kohei Himei

Nakashima Propeller Co., Ltd., Okayama, Japan

ABSTRACT

Surface Piercing Propeller (SPP) is used for the high speed vessels planing to reduce the frictional resistance at the hull of the ship. Thus, SPP works on the particular fully or partially ventilated condition including the free surface problem. This working condition, therefore, makes it hard that SPP designer calculate these propeller open characteristics with high reliability.

In this paper, by conventional theoretical calculations and RANS simulations, the author analyzed propeller open characteristics for the typical SPP which had carried out the model tests. About RANS simulations approach using the Volume of Fluid (VOF) method, in order to keep the computational accuracy including the ventilation behavior and prevent the numerical diffusion, the finely meshes and several calculation conditions were set effectually.

Regarding propeller open characteristics and the rotational fluctuation of 6-component force/moment, the results of RANS/VOF simulations agreed with the experimental measurements well. Moreover, the other calculations for some SPPs which varied these geometrical shapes were also carried out and were estimated the influence on their performances caused by the differences under the free surface condition.

Keywords

Surface Piercing Propeller, RANS simulation, Volume of Fluid method.

1 INTRODUCTION

SPP working under the special condition as partially submerged can achieve high propulsive efficiency on high-speed craft because larger diameter acceptance due to few geometric restriction and the drag reduction of propeller, shaft and other appendages. The blades repeat entry to and exit from the free surface and the suction sides of blades are exposed to ventilated cavitation while it is under the water. In designing SPP, therefore, it is necessary to treat the effects on performances of SPP by this working condition appropriately.

To research about dynamic blade loads, forces, and moments, many model tests on various conditions in free surface tunnel were carried out by Olofsson (1996). And in the way to model the physical phenomena, numerical method using three-dimensional boundary element method was developed by Young & Kinnas (2001).

In this paper, analysis program using potential flow theory for supercavitating propeller was diverted for SPP. On the other hand, higher precision and advanced analysis were carried out by RANS simulations. By developing these two methods, it is expected that SPP's performance and special characteristics can be obtained in a short period of time or with more precision.

2 TARGET SPP

In this work, numerical calculation results for propeller model 841-B were compared with experimental measurements by Olofsson (1996). The photograph and principal particulars of model 841-B are shown in Figure 1 and Table 1. The propeller immersion ratio was defined as Formula (1) below:

$$I = h / D \qquad (1)$$

Where h is the blade tip immersion; and D is propeller diameter as shown in Figure 2. All calculations were carried out at I=0.33 and zero shaft yaw and inclination angle.

Figure 1 Photograph of model 841-B (Olofsson, 1996).

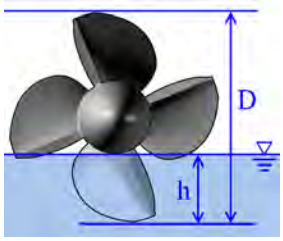

Figure 2 Definition of immersion ratio. (*I=h/D=0.33*)

Table 1 Principal particulars of 841-B

Diameter	250 mm
Hub diameter	85 mm
Pitch at 0.7 radius	310 mm
Pitch ratio at 0.7 radius	1.24
Expanded area ratio	0.58

3 VORTEX LATTICE METHOD

Before the approach using RANS/VOF simulations, the other theoretical calculations were carried out. This computational code using vortex lattice method was developed by Kudo & Ukon (1994) for the analysis of fully submerged supercavitating propeller. It can obtain propeller open characteristics at practicable short times although without the effects by partially submerged condition.

3.1 Calculation Condition

The vapor pressure of water was set the same as the static pressure on water surface in cases of these calculations. It means cavitation number is zero. Cavitation occurred at the blade leading edge easily like ventilated condition. And the pressure of ventilation (cavitation) area on blade suction side and in wake was equal to the static pressure.

3.2 Comparison with Experimental Results

First of all, about propeller open characteristics, advance coefficient J, thrust coefficient K_T, torque coefficient K_Q, and propeller open efficiency η_O were defined as Formula (2), (3), (4), and (5) below respectively:

$$J = V/(nD) \quad (2)$$

$$K_T = T/(\rho n^2 D^4) \quad (3)$$

$$K_Q = Q/(\rho n^2 D^5) \quad (4)$$

$$\eta_O = J \cdot K_T/(2\pi \cdot K_Q) \quad (5)$$

And Froude number based on propeller diameter F_{nD}, Weber number based on propeller diameter W_{nD}, and cavitation number σ were defined as Formula (6), (7), and (8) below respectively:

$$F_{nD} = V/\sqrt{gD} \quad (6)$$

$$W_{nD} = V/\sqrt{\sigma_\kappa/\rho D} \quad (7)$$

$$\sigma = (p_0 - p_v)/(0.5\rho V^2) \quad (8)$$

Where V is Advance speed of propeller; n is Rate of revolution; T is Propeller Thrust; Q is Propeller Torque; ρ is Mass density of water; g is Gravitational constant; σ_κ is Surface Tension of water; P_0 is static pressure on water surface; P_V is vapor pressure of water.

Calculated thrust and torque were several times higher than experimental measurements because propeller was analyzed on fully submerged condition. Hence, these values should be modified to correspond to partially submerged condition. K_T and K_Q, although it is a roughly approximation, were modified by multiplying the conversion factor (=0.288) as shown in Figure 3.

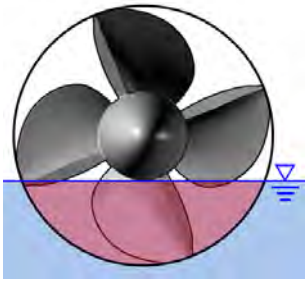

Figure 3 The ratio of area under water to propeller disc. Red painted submerged area is 28.8% of propeller disc area in case of I = 0.33.

Comparison between the calculation and experimental results are shown in Figure 4. Modified K_T and K_Q had passably good agreements with experimental results with the exception of J=1.2. Because the design point (working point) of this SPP seem to be around J=1.0, it may be said that this method to be finished in a very shorter time than RANS simulation is practicable and effective to estimate rough performance or propeller matching at early design phase. However calculated η_O was up to 7% higher than experimental one because increase of K_T was more than K_Q overall.

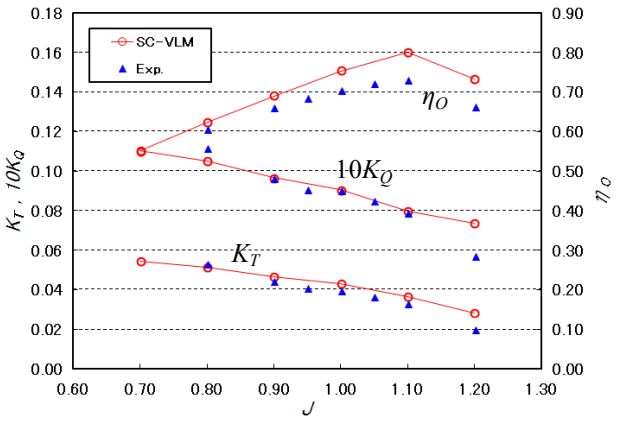

Figure 4 Comparison between the calculated and measured K_T, K_Q, and η_O. (Experiment: F_{nD}=6, σ =2.3)

4 RANS/VOF SIMULATION

RANS simulations were carried out using the commercial CFD software, "SCRYU/Tetra V9". And Volume of Fluid method using interface-volume tracking algorithm was adopted for two-phase flow analyses.

4.1 Calculation Condition

In RANS simulations, large static region and small rotational region were set as shown in Figure 5. Size of these cylindrical regions was set large enough to vanish

the effects on thrust or torque generated by propeller. To be able to evaluate within applicative time with keeping analysis precision, meshes around only key-blade were set more finely than other blades or hub as shown in Figure 6. Especially, meshes where it was expected that ventilation would occur were set more finely. These were around leading edge and trailing edge of blade, the area over suction side, and the wake area as shown in Figure 7. These finely meshes in wake area were extended to half turn from trailing edge of blade to develop the ventilation until blade exit from water. Finally the total number of meshes was about 2.7 million.

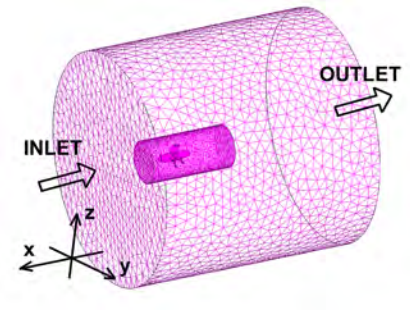

Figure 5 Total meshes for CFD analyses. Ship fixed coordinate system are also shown.

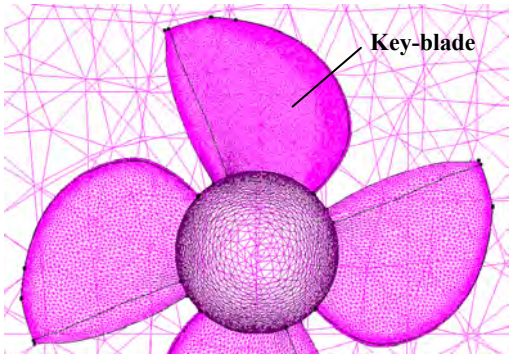

Figure 6 Meshes on key-blade

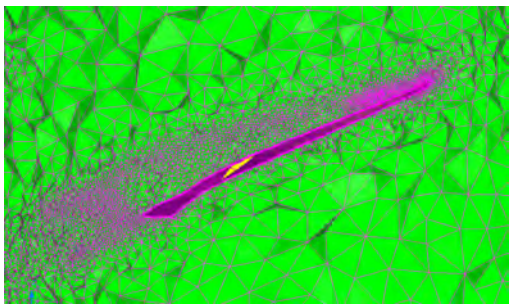

Figure 7 Meshes around key-blade at 0.8 radius.

Table 2 shows about other setting conditions for RANS/VOF simulations. Time step per cycle was always limited to keep Courant number less than 1.0 during calculation. Actually, Courant numbers of each cycle on all simulations remained in the vicinity of 0.4.

For the purpose of comparison with experimental measurements by Olofsson (1994), the flow conditions in each J were set as shown in Table 3. According to Shiba (1953) and Olofsson (1994), the effect of Weber number is negligible when it is sufficiently high as $W_{nD} > 200$. At J=0.4, to reduce the influence of vaporizing cavitation, σ was selected the largest number in the experimental conditions. At other flow conditions, as well as Weber number, the effects of Froude number and cavitation number are negligible and the cavities are fully ventilated. (Olofsson 1994).

Table 2 Setup conditions for RANS/VOF simulations

Turbulent model	MP (Modified Production) k-ε
y^+	100
Time step per cycle	Courant number < 1
Convective term	2nd-order upwind scheme

Table 3 Flow conditions at each J

J	F_{nD}	W_{nD}	σ
0.4	2	237	20.3
0.6	4	475	5.1
0.8	4	475	5.1
1.0	6	712	2.3
1.2	6	712	2.3

The initial interface was set horizontally at the designated immersion ratio. Therefore, in early rotational stage until propeller was rotated several times and the interface deformation was kept stable, the distributions of 6-component force/moment coefficient in each rotation were fluctuated as shown in Figure 8. Each force/moment were transformed to non-dimensional coefficient by divided by $\rho n^2 D^4$ or $\rho n^2 D^5$ respectively as same as K_T and K_Q. In case of Figure 8, only the distributions after fourth rotations (1440 degrees in key-blade angular position) could be evaluated. All results by RANS simulations in this paper were evaluated on the condition that these distributions after several rotations were stable compared with them of previous and next rotation.

4.2 Comparison with Experimental Results

By averaging the distributions of force and moment about x-axis in adoptable some rotations, K_T and K_Q were calculated. Comparison between simulated and measured propeller open characteristics is shown in Figure 9. Similarly, comparisons of 6-component force/moment coefficients at low and high J are shown in Figure 10. Experimental data in Figure 9 and 10 correspond to the flow conditions using for RANS simulations shown in Table 3.

Simulation results had very good agreements with experimental measurements at higher J. Although the absolute value of K_T and K_Q are quite smaller than them of fully submerged propeller, their differences of both results were smaller than 0.007 at J=1.0 and 1.2. Comparison of the observed and simulated ventilated cavity patterns at J=1.0 and 1.2 were shown in Figure 11. In these figures, simulated ventilated cavities were shown as iso-contour that fluid volume fraction was 0.25. Patterns by RANS simulations agreed with observations very well. Because the meshes for only key-blade were finely, however, wake for other blades were not ventilated in simulations.

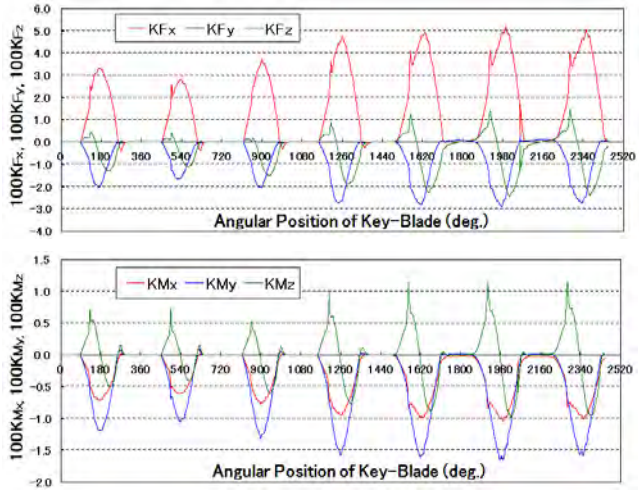

Figure 8 The fluctuations of distributions in early stage. (at J=0.8)

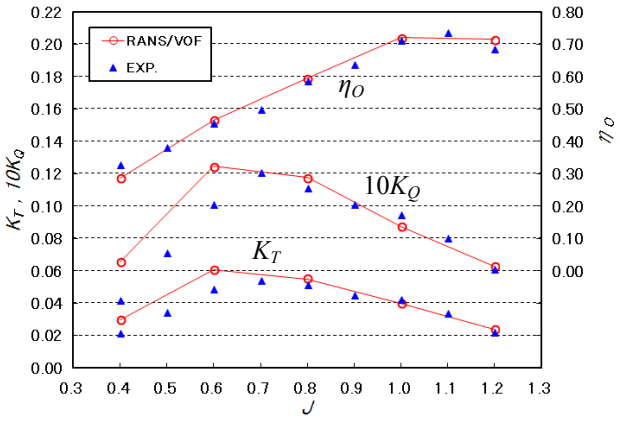

Figure 9 Comparison between the simulated and measured K_T, K_Q, and η_O.

By contrast, good agreement could not have at lower J. Simulated K_T and K_Q were about 30% higher than experimental measurements at J=0.4 or 0.6. In experiment environment, because water had been agitated hard by blades and ventilated cavitation at lower fluid velocity, it may be that the blade working area had been gas-laden multiphase flow not only liquid phase. Hence K_T and K_Q were less than RANS simulations. On the other hand, about RANS simulations, the prominence and depression of the interface were smaller than experiments.

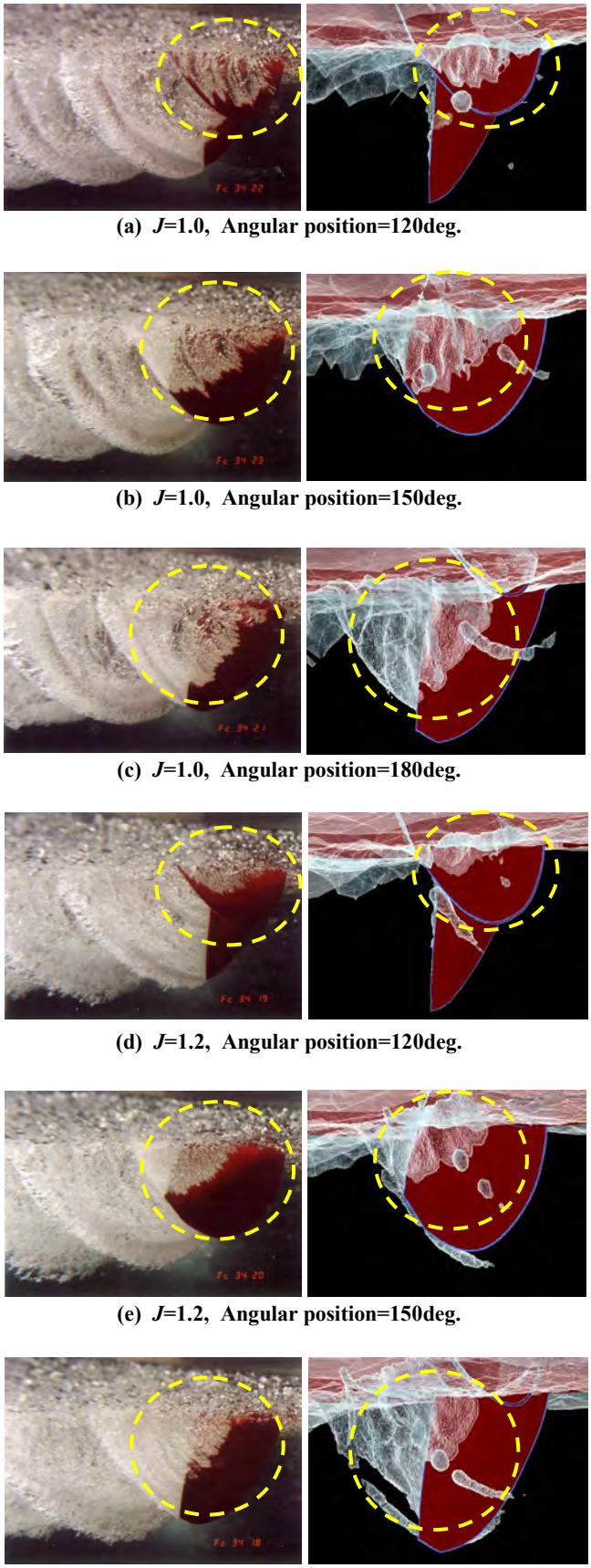

(a) J=1.0, Angular position=120deg.

(b) J=1.0, Angular position=150deg.

(c) J=1.0, Angular position=180deg.

(d) J=1.2, Angular position=120deg.

(e) J=1.2, Angular position=150deg.

(f) J=1.2, Angular position=180deg.

Figure 11 Comparison of the observed and simulated ventilated cavity patterns.

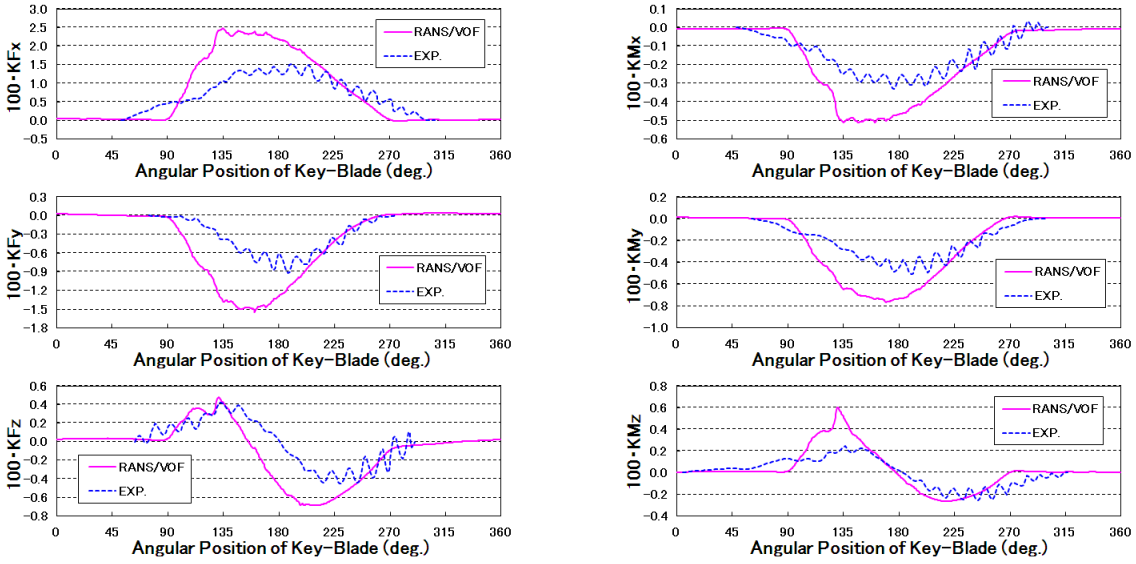

(a) $J = 0.4$

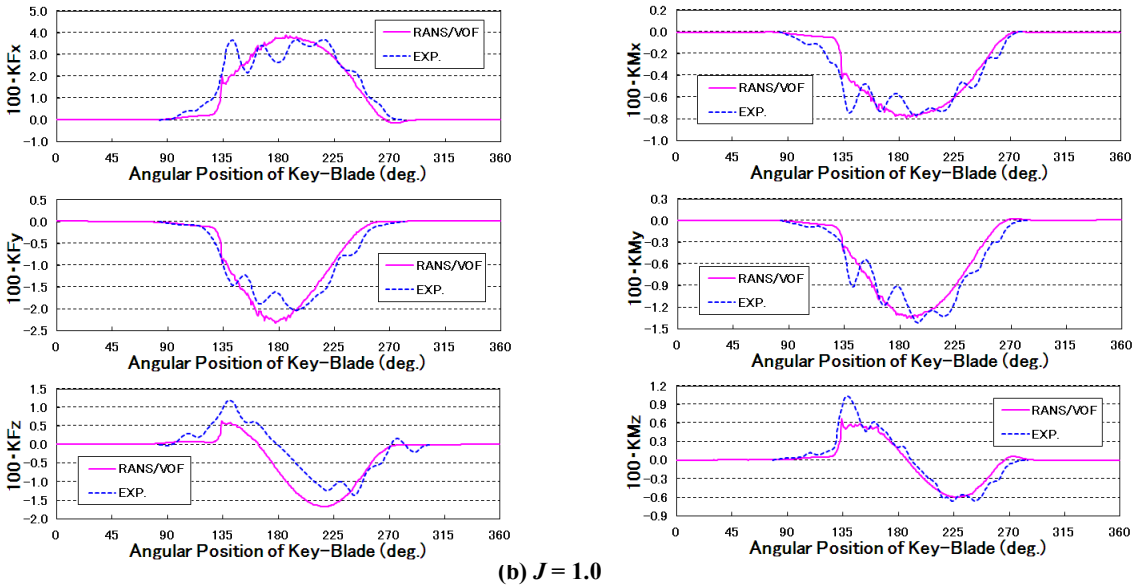

(b) $J = 1.0$

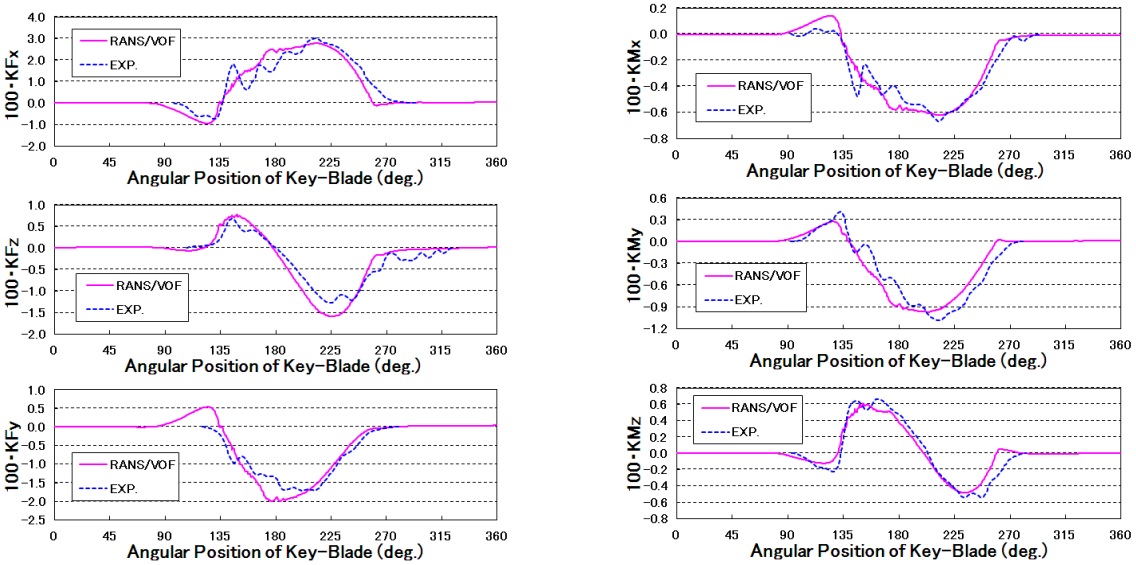

(c) $J = 1.2$

Figure 10 Comparison between the calculated and measured rotational fluctuation of 6-component force/moment.

These differences of interface position are seen by the comparisons of K_{Fx} and K_{Mx} distributions at J=0.4 in Figure 10(a). Thrust and torque started to be generated at larger angular position than experiments. It means that interface transformation level was low and blades enter later and exit earlier than them in experiments. In addition, in VOF method in this work, the liquid phase and the gas phase were separated clearly and it did not treat the multiphase flow. It may be necessary to solve the liquid density depression by intense agitation at lower J.

4.3 Analysis of SPP Series have Varied Number of Blades

Unlike in the case of fully submerged propeller, the effects of principal particulars, for example, even number of blades or expanded area ratio, on SPP's performance have not been investigated theoretically enough. As one of approaches, four SPPs shown in Figure 12, which changed the number of blades from 2 to 5, were analyzed by RANS simulations. These SPPs were designed based on propeller model 841-B. To investigate about effects on partially submerged condition simply, without regarding propeller loads, these SPPs have isometric blades. Thus, 4 blades SPP is the same as propeller model 841-B.

RANS simulations were carried out on flow condition shown in Table 3 at J=0.4. Comparison of K_{Mx} between these SPPs was shown in Figure 13. Regarding the angular range that blade was in the water and generated the hydrodynamic force, 5 blades SPP was shorter than 2 blades SPP slightly. In case that fluid velocity was slower and rate of revolution was higher, namely J was lower, because the interface was dented with the rotation of previous blade and because key-blade entered to this depression, thrust and torque seem to be decreased. The effects of number of blades may be so remarkable compared with fully submerged propeller at lower J.

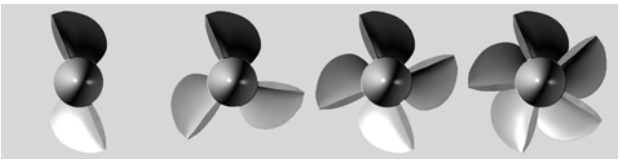

Figure 12 SPP series which changed the number of blades.

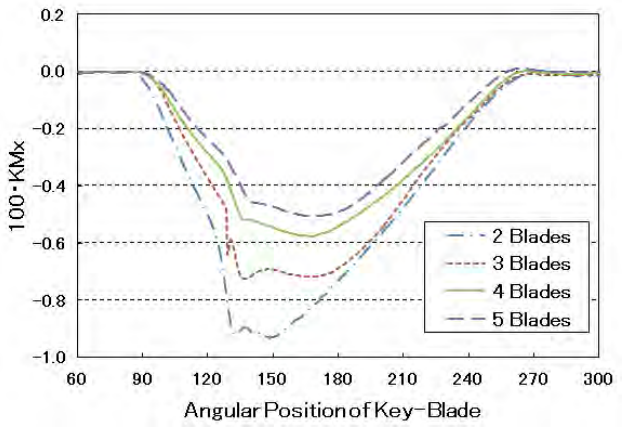

Figure 13 Comparison of K_{Mx} between SPP series

5 CONCLUSIONS

Two theoretical methods for analysis SPP were carried out. One is the diversion of program code for supercavitating propeller using vortex lattice method and the other is RANS simulation applied VOF method. Main conclusions which were obtained in this paper are as follows;

- Even the analysis program for fully submerged supercavitating propeller could analyze SPP reasonably by simple adjustment of calculated results with considering the immersion ratio of SPP.
- RANS simulations had good agreement with experimental results. At lower J, although, the differences of both were larger than at higher J because the interface position and conditions of liquid and gas phases might not be matched with experiments.
- The effects of number of blades seem to be greater than fully submerged propeller especially at lower J.

ACKNOWLEDGEMENT

This work is a part of study as author's doctor course in the University of Tokyo. The author would like to sincerely thank Prof. Yamaguchi for his valuable guidance and insightful comments.

REFERENCES

Kudo, T. and Ukon, Y. (1994). 'Calculation of Characteristics of Supercavitating Propeller Performance Using Vortex Lattice Method'. Proceedings of The 2nd International Symposium on Cavitation, Tokyo, Japan, pp.403-408.

Olofsson, N. (1996). 'Force and Flow Characteristics of a Partially Submerged Propeller'. PhD thesis, Department of Naval Architecture and Ocean Engineering, Chalmers University of Technology, Göteborg, Sweden.

Shiba, H. (1953). 'Air-Drawing of Marine Propellers'. Technical Report 9, Transportation Technical Research Institute, Japan.

Young, Y. L. & Kinnas, S. A. (2001). 'Numerical Modeling of Supercavitating and Surface-Piercing Propeller Flows'. In: CAV 2001: Fourth International Symposium on Cavitation, California Institute of Technology, California, USA.